Non-Covalent Functionalization of Individual Nanotubes with Spiropyran-Based Molecular Switches

Antonio Setaro, Pascal Bluemmel, Chandan Maity, Stefan Hecht,* and Stephanie Reich*

Single-walled carbon nanotubes (SWCNTs) are functionalized with a spiropyran derivative, which is attached non-covalently to the SWCNT's sidewall via a pyrene anchor group. Using this non-covalent functionalization strategy, individual SWCNTs can be stabilized in solution without the need for additional surfactants. Bright luminescence confirms the presence of individual tubes in the thus-prepared samples. In these samples, the majority of pyrene-spiropyran molecules are attached to the walls of the SWCNTs. Upon complex formation with the SWCNT, the switching moiety retains its ability to switch, i.e., to undergo reversible transformations between the closed spiropyran and the opened merocyanine form, and is stable over many cycles of operation.

1. Introduction

Single-walled carbon nanotubes (SWCNTs) are cylinders made out of graphene sheets cut and rolled up along a certain direction described by a chiral vector $\vec{c} = \{n_1, n_2\}$, where n_1 and n_2 are the number of unit cells along the two base directions in the honeycomb crystal lattice of graphene. Depending upon their chirality, SWCNTs show different properties; for example they can be semiconducting or metallic. As a consequence of their quantum nature, they exhibit remarkable optical, mechanical, and transport properties.[1] Often, however, it is desirable to further tailor their properties by functionalization.[2–5] Functionalization can be used to isolate and suspend tubes,[6] to select certain chiralities out of bulk samples[7–9] or to alter their electronic and optical properties.[4,10] Particularly interesting are functionalization schemes, which confer an additional element of control over the SWCNTs' properties, e.g., by decorating the SWCNTs with stimuli-responsive moieties.[11] Due to its high spatiotemporal resolution and its non-invasive nature, light serves as one of the most advantageous external stimuli. Hence, molecular switches,[12] which are able to reversibly undergo optically triggered transitions between two or more metastable states associated with different physicochemical properties, are particularly attractive to control the properties of materials.[13] Among such photochromic compounds, spiropyrans (SPs) offer the unique possibility to change the dipole moment dramatically (by more than 10 D) upon light-induced conversion of the charge-neutral, colorless SP to its corresponding zwitterionic, colored merocyanine (MC) valence tautomer. In 1952 Fischer and Hirschberg[14] predicted the potential of SPs for memory applications,[14] yet thus-far SPs have technologically been implemented primarily in photochromic lenses. The SP-MC system was recently proposed as key element for controlling the emission of fluorophores to enable super-resolution imaging methods.[15]

In the context of SWCNTs, nondestructive functionalization schemes for bulk quantities of nanotubes prove difficult to develop. Previous attempts used covalent functionalization routes to attach the SP switches via a tether to the SWCNTs' walls.[16,17] The covalent attachment strongly alters the electronic properties of the SWCNTs; it degrades the bright and narrow luminescence of the tubes as well as their low-energy ballistic electron transport. Other functionalization schemes[16] targeted SWCNT bundles, which differ very strongly in their properties from individual SWCNTs; in particular, nanosized effects are blurred out.[1,18] Studies on non-covalently SP decorated SWCNTs presented functionalization schemes for single, individual nanotubes that were already isolated on a substrate. Studies of individual SWCNT species, however, are unable to use the confinement-size relation of nanotubes for tailoring their properties and unsuitable for further optimization, e.g., by looking at various SWCNT species (chiralities).

Here, we demonstrate the non-covalent attachment of SP photochromes to individual SWCNTs in solution ensuring preserving the 1D nature of SWCNTs. Our method shows the route for routine stabilization and functionalization of individual SWCNTs in solution starting from bulk samples of as-grown carbon nanotubes. The photoswitches are attached to the nanotube sidewalls via pyrene anchoring groups, without making use of additional surfactants. To optimize the interaction between the induced MC dipole moment and SWCNTs, we chose to attach the pyrene anchor to the N-atom of the SP to allow for coplanarity of the MC and its dipole with the nanotube axis. This is in contrast to the approach followed by Nuckolls

---

Dr. A. Setaro, P. Bluemmel, Prof. S. Reich
Department of Physics of the Freie Universität Berlin
Arnimallee 14, 14195 Berlin
E-mail: setaro@physik.fu-berlin.de

C. Maity, Prof. S. Hecht
Department of Chemistry of the Humboldt-Universität zu Berlin
Brook-Taylor-Str. 2, 12489 Berlin
E-mail: sh@chemie.hu-berlin.de

DOI: 10.1002/adfm.201102451

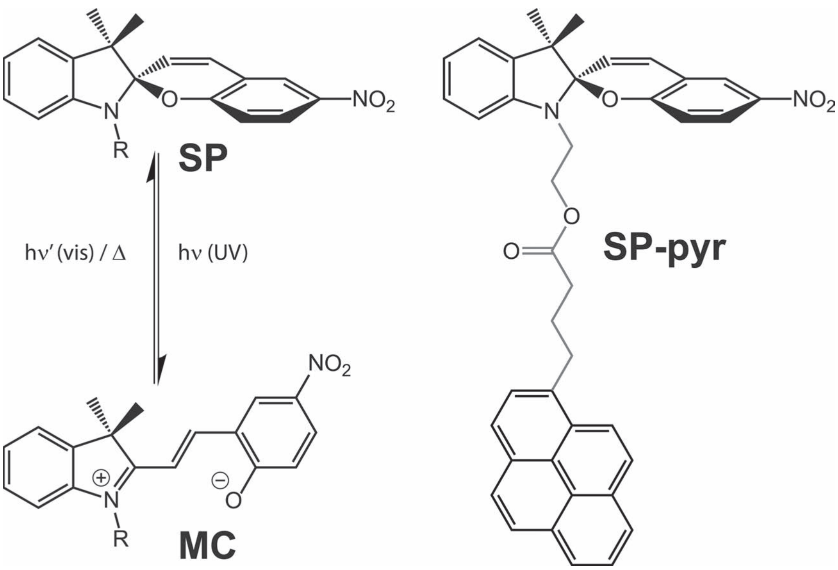

Figure 1. Molecular structures of SP and its corresponding MC (left) as well as molecular structure of the investigated SP-pyr (right).

and co-workers, who attached the pyrene anchor group to the indole backbone in para-position of the N-atom.[19] We expect this choice of coplanar configuration to maximize the interaction between the π-orbital of the ring-open merocyanine form and the extended π-orbital network of the nanotubes. The thus functionalized SWCNTs are well soluble in organic solvents and their dispersions remain stable over long periods of time. Our approach preserves the 1D nature of the pristine nanotubes as demonstrated by photoluminescence experiments, which are the first of their kind for SWCNT samples functionalized with photochromic dipole switches. Most importantly, reproducible and rapid light-induced switching between the ring-closed SP and ring-open MC forms could be achieved, characterized by fast response times and fully reversible switching cycles.

2. Molecular Design and Synthesis of the Spiropyran-Pyrene Dyad

Photochromic SP molecules[20] feature an indole and a benzopyran moiety, which are joined together at the spiro sp^3-hybridized carbon atom that leads to a perpendicular orientation of both planar heterocyclic rings (**Figure 1**). Absorption of UV photons leads to formation of the corresponding MC form (Figure 1) accompanied by breaking of the carbon–oxygen bond and conversion of the spiro-center to an sp^2-hybridized carbon atom, which allows both heterocyclic moieties of the molecule to become coplanar. This in fact leads to an extended π-conjugated system associated with a new absorption band centered in the visible range of the spectrum around 600 nm. Due to its zwitterionic character, the MC form is much more polar as compared to the SP form, giving rise to a large dipole moment ranging from 10 D to 15 D.[21–23]

In order to attach the SP moiety to the SWCNT, a non-covalent approach was chosen as it allows for facile modification of the tubes without compromising for loss of their advantageous electronic properties.[24] For this purpose a pyrene fragment, which has been proven[25] to efficiently stick on the nanotubes sidewalls, was attached as an anchoring group to the SP moiety via a flexible linker as illustrated in the chemical structure of the spiropyran-pyrene dyad (SP-pyr; Figure 1). Note that both linker length as well as the relative orientation of the SP and MC forms to the SWCNTs were carefully taken into account. While the groups of Haddon[16] and Giordani[17] used extremely short (0.5 nm) and long (2.5 nm) linkers, respectively, we chose an intermediate linker length and attached it to the N-atom of the SP to allow for coplanarity of the MC and its dipole with the nanotube axis as opposed to attaching it to the indole backbone as reported by Nuckolls and co-workers.[19]

The desired spiropyran-pyrene dyad SP-pyr was synthesized by esterification of pyrene-1-butyric acid with 1-(2-hydroxyethyl)-3,3-dimethyl-6′-nitro-indolespirobenzopyran, which was obtained from 2,3,3-trimethylindoline via alkylation with 2-bromoethanol, followed by treatment with aqueous sodium hydroxide and subsequent condensation with 5-nitro-2-hydroxybenzaldehyde (see Supporting Information).

3. Switching Behavior of the Spiropyran-Pyrene Dyad

The absorption spectra of SP-pyr in tetrahydrofuran (THF) solution are a superposition of the absorption spectra of its individual components, i.e., pyrene-1-butyric acid and 1-(2-hydroxyethyl)-3,3-dimethyl-6′-nitroindolespirobenzopyran (see Supporting Information). Hence, to a first approximation there is negligible interaction between the spiropyran and pyrene moieties in the ground state. Irradiation of SP-pyr in THF solution with light of 350 nm wavelength leads to formation of a photoproduct with a strongly bathochromically shifted absorption band centered at around 570 nm, characteristic for the MC form (**Figure 2**). In the MC form, the characteristic absorption bands of the pyrene anchoring group remain unchanged, verifying that the photoreaction occurred in the SP moiety. Over time, the absorption spectra revert back to the original spectrum, indicative of the thermally triggered MC → SP conversion (Figure 2). Most importantly, these transformations between the ring-closed SP isomer and the ring-opened MC isomer are almost fully reversible (Figure 2).

4. Characterization of SWCNTs Functionalized with SP-pyr

The photoluminescence of the spiropyran-functionalized nanotubes (**Figure 3**) is characterized by several peaks of high intensity in the excitation versus emission plot that correspond to semiconducting nanotubes of different (n_1,n_2) type

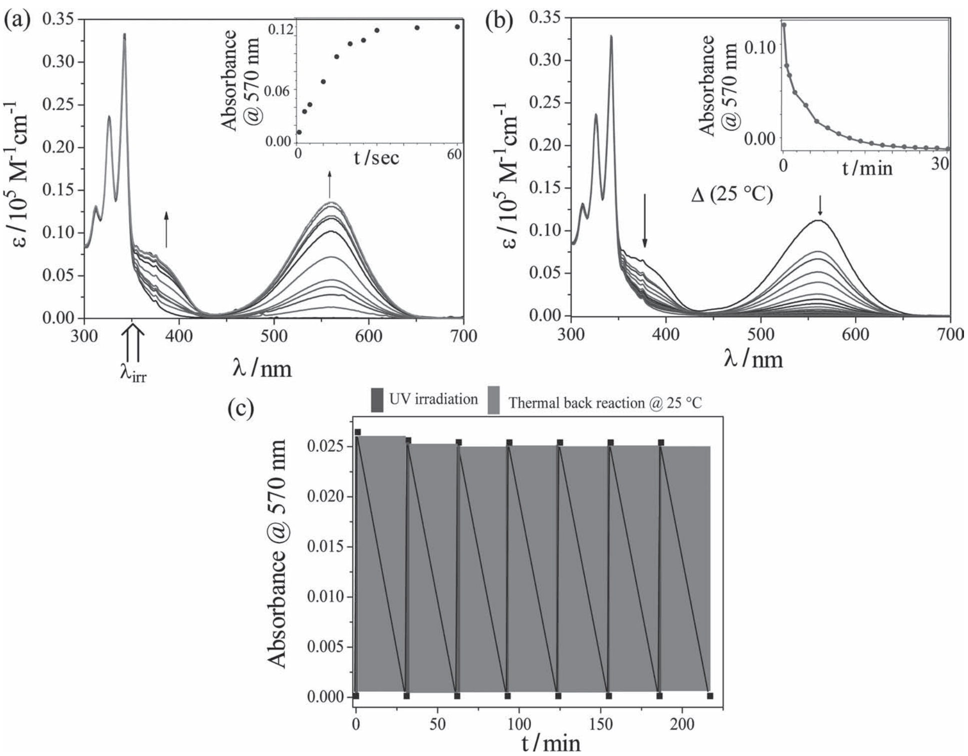

Figure 2. Switching behavior of SP-pyr in solution: a) UV-vis spectra of SP-pyr in THF (concentration $c = 1 \times 10^{-5}$ M) during irradiation with light of 350 nm wavelength. The inset shows plot of absorbance at 570 nm vs. time. b) UV-vis spectra of SP-pyr in THF ($c = 1 \times 10^{-5}$ M) during thermal back reaction at 25 °C. The inset shows the plot of absorbance at 570 nm vs. time. c) Reversible modulation of absorption intensity at 570 nm for photochemical forward and thermal back reaction over several switching cycles.

(chirality).[1] Bright luminescence is generally accepted as proof of a successful debundling and isolation of carbon nanotubes in solution.[26,27] Otherwise, the metallic tubes in a bundle quench the excitation without emitting any photons. Our preparation procedure exploited only the SP-pyr compound without using additional surfactants. The compound thus attached to the nanotube surface and prevented rebundling. To our knowledge this is the very first report of successful debundling of carbon nanotubes with a dipole switch derivative. Debundling is a key requirement for investigating the influence of the switching dipole moment on the nanotube properties.

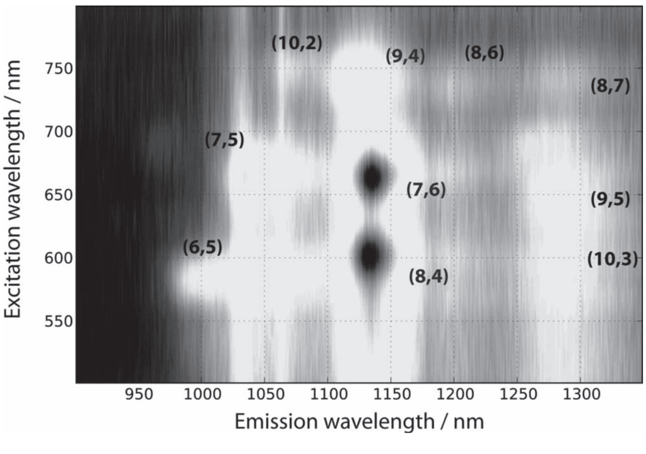

Figure 3. Photoluminescence emission map of a dispersion of the SWCNTs and SP-pyr in THF (SWCNT: 0.01 g L^{-1}, SP-pyr: 5 µM). The plot shows the emission intensity as a function of both excitation and emission wavelength. The maxima were assigned to the nanotube chiralities following the procedure of ref. [26,27].

Subsequently, the adsorption of the SP-pyr to the sidewall of the nanotube was analysed using photoluminescence. **Figure 4**a shows the emission of the SP-pyr solution before adding any nanotubes. Two features can be recognized: First, the pyrene luminescence shows an emission between 350–450 nm and an excitation range 300–360 nm. Second, a signal from the merocyanine open form of the dipole switch can be observed; its emission range is 600–700 nm, the excitation 360–400 nm. After carbon nanotubes were added to the solution, the luminescence signal shown in (Figure 4b) was obtained. Importantly, no pyrene emission is detected after the introduction of nanotubes. This suggests a quenching of the pyrene emission upon the attachment to the tube, most likely by an electron transfer from the pyrene to the nanotube. Unbound SP-pyr will remain emissive but the fraction of free molecules in solution appears to be very small as compared to the fraction of adsorbed molecules. Interestingly, the luminescence of the merocyanine molecule is only weakly affected by the presence of the tubes. Due to the presence of the linker the spiropyran/merocyanine part of SP-pyr is well separated from the pyrene anchor group (1 nm), responsible for the remaining

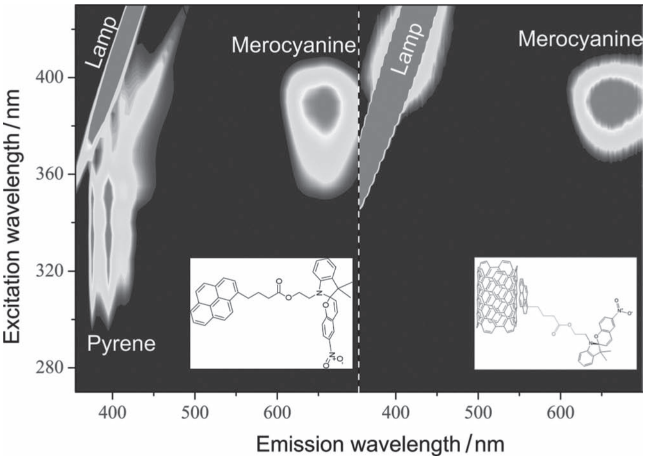

Figure 4. Photoluminescence emission map in the UV excitation range of the pyrene-spiropyran SP-pyr in THF solution in the absence (a) and presence (b) of SWCNTs. The respective insets show the molecular configuration of the free SP-pyr (a) and of the SP-pyr functionalized tubes (b).

luminescence of the merocyanine, which in fact is a first indication that switching might persist in SP-pyr functionalized nanotubes.

To gain quantitative insight into the SP-pyr adsorption to the tubes, the intensity of the pyrene emission excited at 340 nm was analyzed (**Figure 5**). While curve (a) in (Figure 5) shows the emission of the free pyrene moiety of SP-pyr before nanotube addition, curve (b) was obtained after adding nanotubes. Upon SWCNT addition there is negligible emission from free pyrene, note that curve (b) was magnified by a factor of 500 to enhance visibility. The vanishing luminescence intensity suggests that most of the pyrene is attached the nanotube sidewalls. Pyrene emission is largely quenched as its excitation is non-radiatively dissipated by the interaction with the tubes, most likely by photoinduced electron transfer from pyrene to SWCNT followed by back transfer. An alternative explanation is that the entire SP-pyr molecule was lost during the nanotube functionalization. To rule out this explanation the intensity of the merocyanine absorption has been compared before and after nanotube addition. This serves as an upper limit of the fraction of SP-pyr molecules left after the functionalization process.

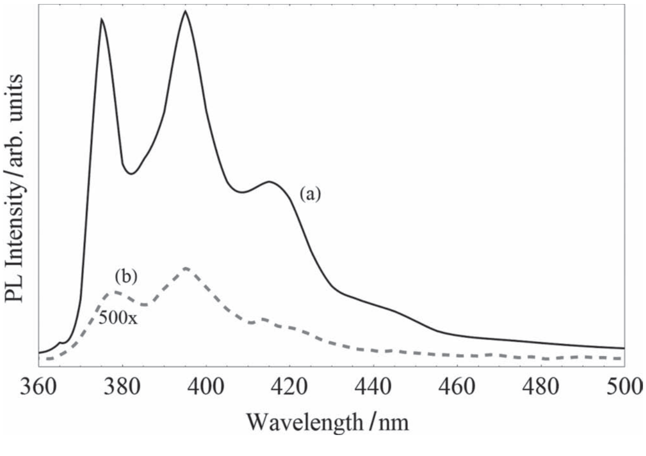

Figure 5. Emission from the pyrene-spiropyran SP-pyr dissolved in THF in the absence (a, solid black line) and in the presence (b, dashed gray line) of SWCNTs. The latter curve (b) was magnified by a factor of 500 for better visibility. A wavelength of 340 nm was used for excitation. Both spectra were measured for the same concentration of SP-pyr in the sample.

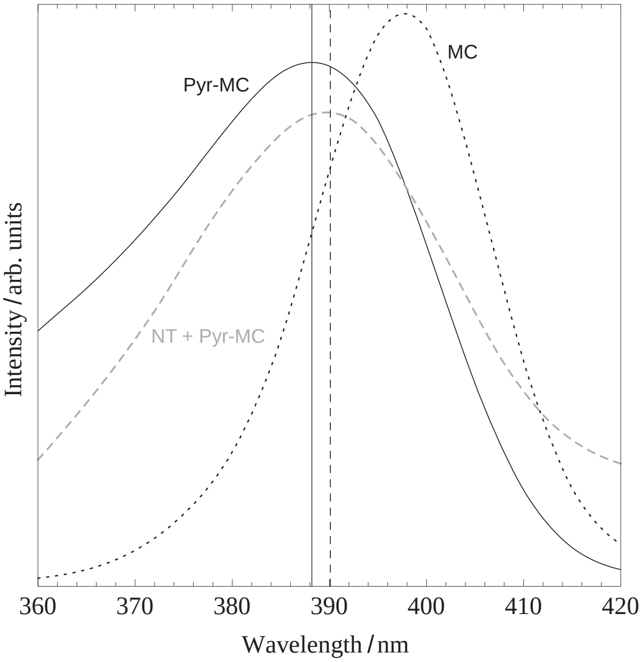

Figure 6. Photoluminescence intensity at 660 nm as a function of excitation wavelength. The spectra were obtained for the merocyanine (MC with $R = CH_2CH_2OH$ shown in Figure 1: dotted line), the pyrene-MC dyad (Pyr-MC: solid line), and carbon nanotubes suspended by the pyrene-merocyanine dyad (SWCNT+Pyr-MC: dashed line). The MC forms were prepared by irradiation of the SP forms.

Instead of absorption spectra, excitation spectra are shown in (**Figure 6**) to deduce the amount of adsorbed pyrene. Hence, the excitation spectra of the free dyad in solution and of the functionalized nanotubes were compared. Furthermore, the excitation spectrum of a 5 μM suspension of the unfunctionalized MC ($R = CH_2CH_2OH$ in (Figure 1a)) in THF is shown for a reference. It can clearly be seen that the MC absorption remains constant during functionalization. To further support our finding we repeated the functionalization (sonication, centrifugation) with identical parameters, but without adding nanotubes to the solution. Without the tubes we obtained identical photoluminescence maps before and after the treatment. This demonstrates that the SP-pyr compound remained stable during the functionalization steps. The vanishing SP-pyr emission cannot be attributed to a degradation of the spiropyran derivative. Hence, there is no loss of the SP-pyr molecules during functionalization. The loss of pyrene emission is clearly caused by their attachment to the nanotube wall. Therefore, the nanotubes are debundled and covered with the SP-pyr compound.

The merocyanine excitation energy shows a slight red shift $\Delta E_{exc} = 10$ meV after the dyad was adsorbed to the nanotubes (Figure 6). This is consistent with the report by Khairutdinov

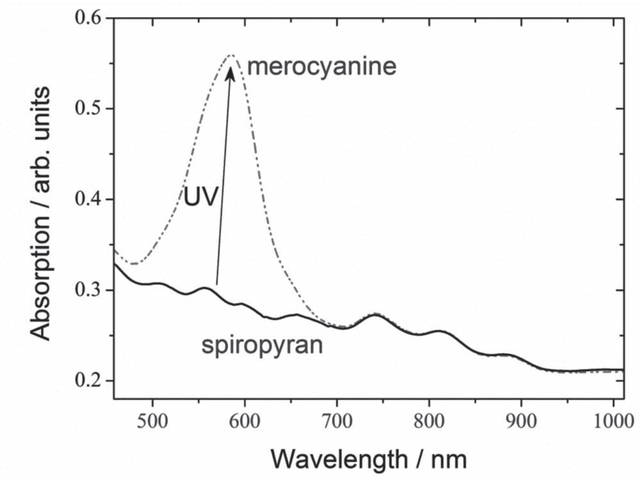

Figure 7. Absorption spectrum of the SWCNT/SP-pyr dispersion in THF before (black solid line) and after irradiation (gray solid line) with UV light (365 nm).

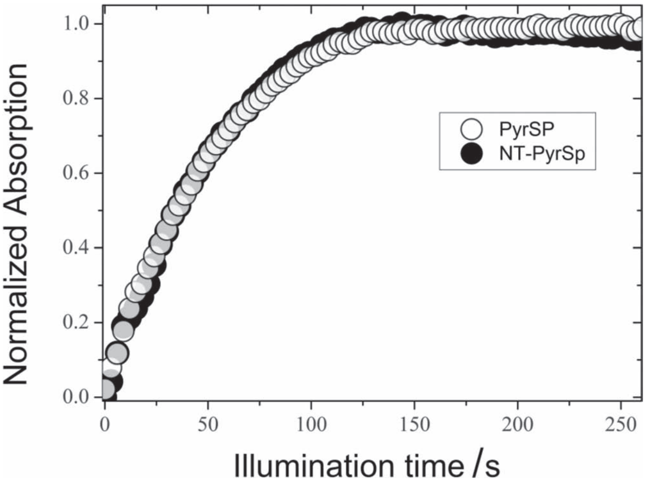

Figure 8. Intensity of the MC absorption band at 590 nm during light-induced ring opening of the SP-pyr dyad in the absence (open circles) and in the presence (black filled circles) of SWCNTs. The curves are normalized to the maximum absorption intensity.

et al.,[16] who observed a shift of 80 meV with a dipole–tube distance of 0.5 nm compared to our distance of 1 nm. MC adsorbed to the surface of bulk materials shows a similar shift,[28,29] which is indicative of the interaction between the MC π-system and the nanotubes.

After verifying the SP-pyr dyad adsorption on SWCNTs, the switching behavior of the SP moiety in the vicinity of the nanotubes was investigated. The standard way of confirming switching is to monitor the intensity of the absorption band at 590 nm, which is the characteristic fingerprint for MC formation. The respective absorption spectrum of the SP-pyr functionalized nanotubes is shown in (**Figure 7**). SP has no absorption features in the visible. The black line in (Figure 7) shows the absorption of the SP-pyr functionalized nanotubes before illumination with UV light. After exposure to UV radiation (365 nm), the dyad converts into the open form and the absorption spectrum (gray dashed line in Figure 7) shows the typical MC absorption band. Hence, our compound retains its ability to switch between the open and closed form on the surface of the nanotubes. Please also note the lack of an absorption feature at 450 nm (extended spectrum available in the Supporting Information), which indicates aggregated MCs and is typically observed in solutions at high concentration.[16] Such absorption band has also been observed after covalent anchoring of merocyanine on carbon nanotubes where it was attributed to the functionalization of the nanotube cap.[16]

The extend of switching was followed by monitoring the merocyanine absorption during the course of irradiation in the absence and presence of SWCNTs (**Figure 8**). The white symbols represent the intensity of the free SP-pyr dyad in solution, the black symbols are for SP-pyr-functionalized nanotubes. The switching dynamics remain unaffected by the interaction of the SP-pyr dyad with the tubes. Furthermore, repetitive switching cycles of alternating ring opening and ring closing transitions were also investigated. The evolution of the 590 nm absorption band of the merocyanine after repeated cycles of UV exposure for ring opening and thermal back reaction in the dark for ring opening (**Figure 9**) proves the reversibility and stability of the switching process over several cycles, which is a fundamental requirement for exploiting such systems in devices.

5. Conclusions

In summary, it has been shown that a SP-based derivative with a pyrene head group attaches to the sidewalls of SWCNTs. The relative orientation between induced dipole moment and SWCNTs axis has been optimized by ensuring coplanarity of the MC dipole moment and the nanotube axis. The SP-pyr molecule stabilizes individual nanotubes in solu-

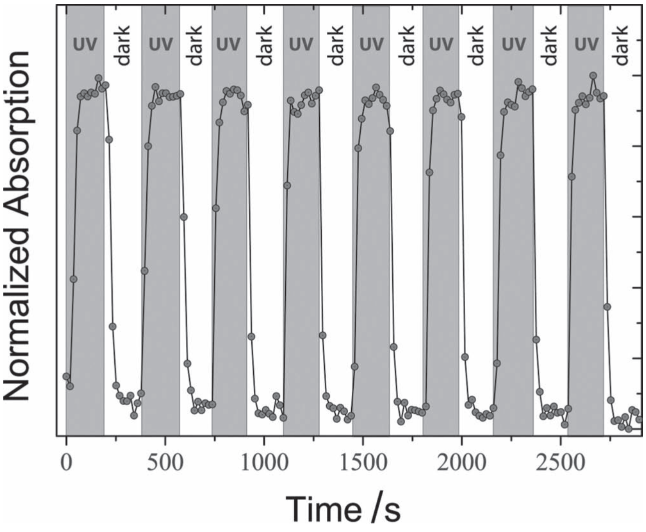

Figure 9. Repetitive switching cycles of photochemically induced ring opening and thermal ring closure of SP-pyr-functionalized SWCNTs monitored by absorption of the MC form at 590 nm.

tion without requiring additional surfactants, which allows for a very straightforward protocol for functionalization of bulk samples of as-grown SWCNTs. This is a major step compared to previous attempts that either targeted single tubes or led to the (covalent) functionalization of nanotube bundles. The attachment of the molecules to the nanotubes has been confirmed by comparing the luminescence intensities of the pyrene anchor that is quenched after functionalization. Likewise, the presence of individual SWCNTs has been confirmed through their bright infrared luminescence, which could be observed and is reported here for the first time for dipole-switch-functionalized SWCNTs. Moreover the repetitive switching between the closed SP and the open MC isomer triggered by UV irradiation and its thermal back reaction was demonstrated. The switching ability was preserved over many cycles of operation. The functionalization of carbon nanotubes with molecular switches allows to reversibly change nanotube properties through irradiation. Further studies are currently underway to investigate the response of the carbon nanotube properties, in particular regarding charge transport, to light-induced changes in the molecular environment, such as local dipole moment changes.

6. Experimental Section

Experimental Setup and Sample Preparation: CoMoCAT nanotubes, produced by SouthWest NanoTechnologies (SWeNT, SG 76), all belonging to the same production batch were used. The tubes had a diameter of 0.9 nm ± 0.3 nm and a high aspect ratio (1000). THF suspensions of the switching compound were prepared setting the molarity to 5 μM. The solution was transparent and exhibited no absorption in the visible. This implies that for THF at room temperature the switch was stable in the SP, ring-closed form. CoMoCAT tubes were added to the solution with a starting concentration of 0.01 g L^{-1}. The mixture was treated with a tip sonicator (Bandelin SonoPlus HD 2070) at a power of 60 W and cycles of 0.5 s. After 1h, the suspensions were centrifuged (Hettig Mikro 220R centrifuge) at 3500 g at 27 °C for 60 min. The collected supernatant was used for the experiments.

Photoluminescence and photoluminescence excitation (PLE) experiments were performed with a Fluorolog-3 Spectrofluometer (Horiba Jobin Yvon). The optical excitation was provided by a xenon lamp with an emission range 240–1000 nm. The light was focused onto the sample; the emission was dispersed in a single-grating spectrometer integrated into the Flurolog and detected with a nitrogen-cooled InGaAs diode array. UV light source was a handheld UV lamp emitting at 365 nm. UV-vis measurements were performed with an Evolution Array Spectrophotometer from Thermo-Fisher, wavelength range 270–1100 nm.

To verify the long-term stability of the samples absorption spectra and PLE maps measured directly after the functionalization and with spectra taken on the same solution two months later were compared. The spectra remained unchanged.

The dispersing ability of the compound was compared with 1-pyrenebutyric acid (CAS # 3443-45-6), which is the commercially available compound morphologically closest to the SP-pyr (essentially the anchoring moiety without the switching part). No significant differences in the intensity of the absorption and luminescence spectra between the two suspensions were observed, suggesting similar dispersing ability.

Statistical AFM Analysis: Statistical atomic force microscopy (AFM) analysis was carried out on a dried sample deposited by spin coating (25 rps) onto a Si/SiO$_2$ (300 nm SiO$_2$ layer thickness). The samples were washed with THF several times after deposition in order to remove excess of surfactant and other impurities. AFM acquisitions were performed with a Park XE-150 AFM microscope operating in the non-contact mode. The mean value of the tubes diameter was 1.37 nm ± 0.02 nm, which very nicely confirmed the photoluminescence results. The histogram of the measured tube diameters is included in the Supporting Information (Figure S8).

Supporting Information

Supporting Information is available from the Wiley Online Library or from the author.

Acknowledgements

Support by the German Research Foundation (DFG via SFB 658, subprojects A6 and B8) as well as the ERC (grant number 210642) is gratefully acknowledged. BASF AG, Bayer Industry Services, and Sasol Germany are thanked for donations of chemicals.

Received: October 11, 2011
Revised: February 3, 2012

---

[1] S. Reich, C. Thomsen, J. Maultzsch, *Carbon nanotubes: basic concepts and physical properties*, Wiley-VCH, Weinheim **2004**.
[2] H. Dai, *Acc. Chem. Res.* **2002**, *35*, 1035.
[3] S. Niyogi, M. A. Hamon, H. Hu, B. Zhao, P. Bhowmik, R. Sen, M. E. Itkis, R. C. Haddon, *Acc. Chem. Res.* **2002**, *35*, 1105.
[4] K. Balasubramanian, M. Burghard, *Small* **2005**, *1*, 180.
[5] D. Tasis, N. Tagmatarchis, A. Bianco, M. Prato, *Chem. Rev.* **2006**, *106*, 1105.
[6] W. Wenseleers, I. Vlasov, E. Goovaerts, E. Obraztsova, A. Lobach, A. Bouwen, *Adv. Funct. Mater.* **2004**, *14*, 1105.
[7] R. Marquis, C. Greco, I. Sadokierska, S. Lebedkin, M. Kappes, T. Michel, L. Alvarez, J. L. Sauvajol, S. Meunier, C. Mioskowski, *Nano Lett.* **2008**, *8*, 1830.
[8] S. Y. Ju, J. Doll, I. Sharma, F. Papadimitrakopoulos, *Nat. Nanotechnol.* **2008**, *3*, 356.
[9] a) A. Setaro, C. S. Popeney, B. Trappmann, V. Datsyuk, R. Haag, S. Reich, *Chem. Phys. Lett.* **2010**, *493*, 147; b) A. Setaro, C. S. Popeney, B. Trappmann, R. Haag, S. Reich, *Phys. Status Solidi B* **2010**, *247*, 2758; c) C. S. Popeney, A. Setaro, R.-C. Mutihac, P. Bluemmel, B. Trappmann, J. Vonneman, S. Reich, R. Haag, *Chem. Phys. Chem.* **2012**, *13*, 203.
[10] P. Bluemmel, A. Setaro, C. S. Popeney, B. Trappmann, R. Haag, S. Reich, *Phys. Status Solidi B* **2011**, *248*, 2532.
[11] E. Malic, C. Weber, M. Richter, V. Atalla, T. Klamroth, P. Saalfrank, S. Reich, A. Knorr, *Phys. Rev. Lett.* **2011**, *106*, 097401.
[12] B. L. Feringa, *Molecular Switches*, Wiley-VCH, Weinheim **2001**.
[13] M.-M. Russew, S. Hecht, *Adv. Mater.* **2010**, *22*, 3348.
[14] E. Fischer, Y. Hirshberg, *J. Chem. Soc.* **1952**, 4522.
[15] B. Seefeldt, R. Kasper, M. Beining, J. Mattay, J. Arden-Jacob, N. Kemnitzer, K. H. Drexhage, M. Heilemann, M. Sauer, *Photochem. Photobiol. Sci.* **2010**, *9*, 213.
[16] R. F. Khairutdinov, M. E. Itkis, R. C. Haddon, *Nano Lett.* **2004**, *4*, 1529.
[17] E. Del Canto, K. Flavin, M. Natali, T. Perova, S. Giordani, *Carbon* **2010**, *48*, 2815.
[18] S. Reich, C. Thomsen, P. Ordejón, *Phys. Rev. B* **2002**, *65*, 155411.
[19] X. Guo, L. Huang, S. O'Brien, P. Kim, C. Nuckolls, *J. Am. Chem. Soc.* **2005**, *127*, 15045.
[20] H. Durr, H. Bouas-Laurent, *Photochromism: molecules and systems*, Elsevier, Amsterdam **2003**.

[21] G. Berkovic, V. Krongauz, V. Weiss, *Chem. Rev.* **2000**, *100*, 1741.
[22] J. A. Delaire, K. Nakatani, *Chem. Rev.* **2000**, *100*, 1817.
[23] V. I. Minkin, *Chem. Rev.* **2004**, *104*, 2751.
[24] A. Hirsch, O. Vostrowsky, *Top. Curr. Chem.* **2005**, *245*, 193.
[25] R. J. Chen, Y. Zhang, D. Wang, H. Dai, *J. Am. Chem. Soc.* **2001**, *123*, 3838.
[26] M. J. O' Connell, S. M. Bachilo, C. B. Huffman, K. L. Rialon, P. J. Boul, W. H. Noon, *Science* **2002**, *297*, 593.
[27] S. M. Bachilo, M. S. Strano, C. Kittrell, R. H. Hauge, R. E. Smalley, R. B. Weisman, *Science* **2002**, *298*, 2361.
[28] K. Sayama, K. Hara, Y. Ohga, A. Shinpou, S. Suga, H. Arakawa, *New J. Chem.* **2001**, *25*, 200.
[29] S. Corni, J. Tomasi, *J. Chem. Phys.* **2002**, *117*, 7266.